Near-infrared photon upconversion devices based on GaNAsSb active layer lattice matched to GaAs

Y. Yang,[1] W. Z. Shen,[1,a)] H. C. Liu,[1,2,b)] S. R. Laframboise,[2] S. Wicaksono,[3] S. F. Yoon,[3] and K. H. Tan[3]
[1]*Department of Physics, Laboratory of Condensed Matter Spectroscopy and Optoelectronic Physics, Shanghai Jiao Tong University, Shanghai 200030, People's Republic of China*
[2]*Institute for Microstructural Sciences, National Research Council, Ottawa K1A 0R6, Canada*
[3]*School of Electrical and Electronic Engineering, Nanyang Technological University, Singapore 639798, Singapore*

(Received 30 December 2008; accepted 7 February 2009; published online 4 March 2009)

Room-temperature full GaAs-based near-infrared (NIR) upconversion has been demonstrated by connecting lattice-matched GaNAsSb/GaAs *p-i-n* photodetectors in series with commercial GaAs/AlGaAs light-emitting diodes (LEDs). Due to the avalanche gain in GaNAsSb/GaAs photodetectors and high internal efficiency in GaAs/AlGaAs LEDs, the upconversion efficiency of the integrated system reaches 0.048 W/W under −7 V bias, much higher than any existing NIR upconverters without amplifying structures. We have further investigated the dependence of the upconversion efficiency on applied bias and incident light intensity. The present work establishes an experimental base for direct epitaxial growth of full GaAs-based NIR upconverters with high upconversion efficiencies. © *2009 American Institute of Physics*. [DOI: 10.1063/1.3091402]

Near-infrared (NIR) upconversion from the eye-safe region (about 1.2–1.6 μm) to shorter wavelength (below 1 μm) has attracted much interest due to its potential applications in many fields such as night vision, range finding, homeland security, and semiconductor wafer inspection.[1–4] The early achievements on the NIR upconversion were demonstrated on Ge/GaAs heterojunction structures[5] and rare-earth ion doped systems.[6,7] In 2000, Liu *et al.*[8] proposed another upconversion mechanism by employing semiconductor structures which is composed of two major parts, a photodetector and a light-emitting diode (LED). A room-temperature NIR upconverter was fabricated by growing both parts (InGaAs/InP photodetector and InAsP/InP LED) on InP substrate.[8] However, the upconversion efficiency was low (<0.0005 W/W) since the LED internal quantum efficiency was limited by the energetic barrier and poor carrier confinement in the InAsP/InP LED active region.

GaAs/AlGaAs LED is capable of much higher internal efficiency and could be employed instead of the low efficiency InAsP/InP LED. However, the lattice mismatch between the GaAs substrate and InGaAs detector active layer increases rapidly with indium content,[9] making it difficult to grow InGaAs/InP photodetector working with GaAs/AlGaAs LED in the eye-safe region through direct epitaxial growth. To bypass this problem, InGaAs/InP photodetector and GaAs/AlGaAs LED were bonded through wafer fusion, an advanced processing technology used for integrating heterogeneous semiconductor materials regardless of their lattice mismatch. This approach turned out to be quite effective and the upconversion efficiency was significantly improved (~0.018 W/W).[10] It should be noted; however that wafer fusion is a specialized processing technique with its own process limitations and challenges,[11] which makes this technology less attractive.

The next significant progress of the NIR upconversion technology is to realize a full GaAs-based approach, i.e., taking advantage of the mature GaAs material to grow both the photodetector and LED on GaAs substrate via epitaxial growth integration. It has been found that the incorporation of a small amount of nitrogen into InGaAs or GaAsSb material can reduce the band gap as well as lattice constant.[12–14] GaInNAs/GaAs (Refs. 9, 15, and 16) and GaNAsSb/GaAs (Refs. 17 and 18) photodetectors operating at 1.3 μm or even longer wavelengths that are lattice-matched to GaAs have been fabricated. For a well-designed GaAs/AlGaAs LED, the internal efficiency can be nearly 100%,[10] which would lead to high upconversion efficiency in full GaAs-based NIR upconverters. In this letter, we report on the demonstration of room-temperature full GaAs-based NIR upconversion by connecting a GaNAsSb/GaAs photodetector in series with a commercial GaAs/AlGaAs LED. Our preliminary study on the upconversion efficiency has shown that the GaAs-based NIR upconverter has the potential of reaching high upconversion efficiencies (>0.04 W/W).

The GaNAsSb *p-i-n* photodetector samples were grown by molecular beam epitaxy on semi-insulating GaAs substrates. The active region of the photodetectors is a 5000 Å thick GaNAsSb layer that is sandwiched between two undoped 500 Å thick GaAs layers. Both *p* and *n*-type contacts are 4000 Å thick GaAs layers, with the former doped with C to a density of 5×10^{19} cm^{-3} and the latter doped with Si to a density of 5×10^{18} cm^{-3}. All layers were grown at a rate of 1 μm/h. To determine the N and Sb content in GaNAsSb, a 100 nm thick GaNAsSb layer was grown on the GaAs substrate, followed by a 100 nm thick GaAsSb layer with identical Sb flux. High resolution x-ray diffraction (XRD) rocking curve on the (004) plane of the sample [Fig. 1(a)] reveals that the signal of the GaNAsSb peak overlaps with the GaAs substrate signal, indicating close lattice matching between the GaNAsSb layer and the GaAs substrate. Through the simulated curve, the N and Sb proportions have been deter-

a)Electronic mail: wzshen@sjtu.edu.cn.
b)Electronic mail: h.c.liu@nrc.ca.

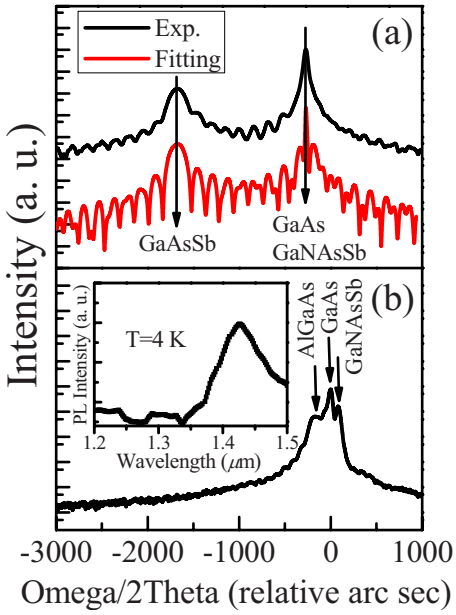

FIG. 1. (Color online) (a) Measured and fitted x-ray rocking curves for 100 nm thick GaAsSb/GaNAsSb two-layer structure on GaAs substrate and (b) measured x-ray rocking curve for GaNAsSb layer on GaAs substrate. The inset of (b) presents the low-temperature PL spectrum of the GaNAsSb layer.

mined to be about 3.3% and 8.0%, respectively, under the assumption that the Sb concentration in both the GaAsSb and GaNAsSb layers are the same. Identical GaNAsSb growth conditions were used during the *p-i-n* photodetector active layer growth. Figure 1(b) shows the XRD rocking curve of the *p-i-n* photodetector sample, which exhibits a minimal separation between the GaNAsSb and GaAs peaks equivalent to ~500 ppm lattice mismatch. The band gap of the GaNAsSb active region has been estimated to be 0.88 eV from the low-temperature photoluminescence (PL) spectrum shown in the inset of Fig. 1(b).

The GaNAsSb *p-i-n* photodetectors were fabricated by using standard photolithographic and wet chemical etching techniques with square mesa sizes of between 400 and 1000 μm. Figure 2(a) presents the room-temperature current-voltage (*I-V*) characteristics of the GaNAsSb/GaAs photodetector with a mesa size of 400×400 μm^2, where the black curve represents dark current and the red one recorded *I-V*, when the detector is illuminated by a 1.3 μm laser diode. Measured dark *I-V* characteristics exhibit good uniformity across different sizes of devices. The two curves in Fig. 2(a) overlap with each other under forward biases, indi-

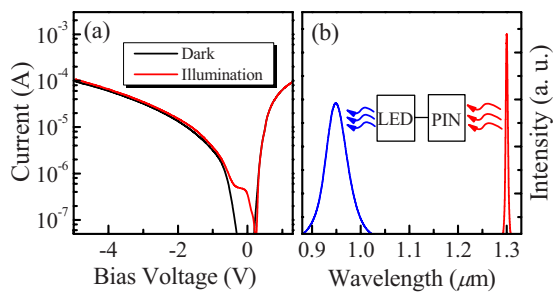

FIG. 2. (Color online) (a) Room-temperature dark and illumination *I-V* characteristics of the GaNAsSb/GaAs *p-i-n* photodetector and (b) schematic experimental setup and the results to demonstrate the upconversion from 1.3 μm laser light to 0.95 μm LED emission.

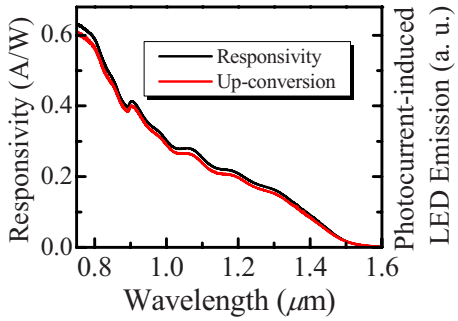

FIG. 3. (Color online) Room-temperature spectral response of the GaNAsSb/GaAs *p-i-n* photodetector and dependence of photocurrent-induced LED light emission of the upconverter on incident light wavelength.

cating small photocurrent there. In contrast, the photocurrent is much larger when the bias voltage is negative, confirming that the detector should be reverse biased during operation. It should be noted that the detector produces a photocurrent of 3.6×10^{-7} A under zero bias and therefore this GaNAsSb-based *p-i-n* acts as a photovoltaic detector. To unambiguously demonstrate the concept of room-temperature full GaAs-based NIR upconversion, we have connected the GaNAsSb/GaAs *p-i-n* photodetector in series with a commercial GaAs/AlGaAs LED. As shown in Fig. 2(b), incident radiation from the 1.3 μm laser diode is absorbed by the GaNAsSb/GaAs photodetector, generating a photocurrent which drives the GaAs/AlGaAs LED to emit strong 0.95 μm infrared light, where the LED emission enhances obviously with the increase in laser illumination upon the photodetector.

In addition to the sensitivity to laser excitation, we have further shown that the NIR radiation from the internal white light source of a commercial Fourier transform infrared spectrometer (FTIR) (Nicolet Nexus 870) can be upconverted, reproducing the FTIR spectral response. The black curve in Fig. 3 is the spectral response of the GaNAsSb/GaAs photodetector under −3 V reverse bias. The spectrum has been performed in the FTIR and corrected by a DTGS TEC detector which has a nearly flat response in the NIR region and further calibrated with the help of the 1.3 μm laser diode. It is clear that the GaNAsSb/GaAs photodetector has an effective detection range between 0.75 and 1.50 μm. The detector responsivity is 0.20 A/W at 1.3 μm for an input incidence of 12 mW/cm^2, while decreases with increasing wavelength and becomes smaller than 0.005 A/W beyond 1.55 μm. The steeper increase shorter than about 0.9 μm is attributed to bulk GaAs absorption. As a preliminary study, the *p-i-n* photodetector is not optimized for the interested 1.2–1.6 μm region. Further improvements are clearly called for. We believe that the key improvement will come with the maturity of this nitride materials system. Moreover, for a specific application, one may enhance the response substantially at a given wavelength by incorporating a resonant cavity.

The red curve in Fig. 3 is the measured dependence of the photocurrent-induced GaAs/AlGaAs LED emission on the wavelength of incident light, i.e., the upconversion spectrum. The input radiation from the internal white light source of the FTIR is shone onto the GaNAsSb/GaAs photodetector, while the output GaAs/AlGaAs LED emission is collected by a Si detector, the signal from which is fed back to the FTIR for data processing. The raw data is then corrected in

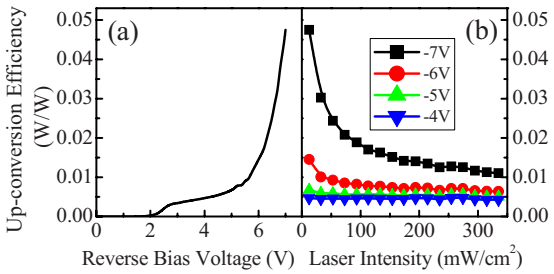

FIG. 4. (Color online) Dependence of room-temperature upconversion efficiency on (a) bias voltage and (b) incident laser intensity.

the same way as before. Near perfect agreement between the spectral response of the photodetector and the upconversion spectrum is observed. As we know, the LED emission intensity is proportional to the injection current. This agreement can be explained by the fact that the LED emission depends only on the photocurrent from the GaNAsSb/GaAs photodetector.

We now estimate the room-temperature upconversion efficiency of the integrated upconverter. The commercial GaAs/AlGaAs LED emits light in all directions, making it difficult to measure the total output power and as a result, the upconversion efficiency. However, we can estimate the full GaAs-based NIR upconverters using typical parameters of GaAs/AlGaAs LEDs as in other NIR upconverters. For injection current density range around 0.1 A/cm^2 which is the case of our device, 100% LED internal efficiency is assumed.[10] The upconversion efficiency is calculated under the assumption of 2% escaping probability of the photons from LEDs.[19] Figure 4(a) shows the dependence of the room-temperature upconversion efficiency for 12 mW/cm^2 incident illumination of the 1.3 μm laser diode on reverse bias voltages across the upconverter. To prevent device damage, we have not biased higher than -7 V. It is found that the upconversion efficiency is negligible for low bias voltages but it exhibits a turn-on behavior at about -2 V and begins to increase. The enhancement is slow for bias voltages between -3 and -5 V where the upconversion efficiency is about 0.0043 W/W.

Further increase in the reserve bias results in a significant enhancement in the upconversion efficiency with no signs of saturation. The responsivity of the GaNAsSb/GaAs photodetector reaches 1.8 A/W at -6 V bias, much higher than the theoretical limit when all incoming photons are absorbed and converted to photocurrent, indicating the existence of avalanche gain, which is consistent with previous observation on these photodetectors.[18] Avalanche effect in the GaNAsSb/GaAs structure can be attributed to the high impact ionization coefficient resulted from midgap As antisite defects. With the avalanche effect, the upconversion efficiency reaches 0.048 W/W at -7 V. In comparison, the upconversion efficiency of the full InP-based NIR upconverter is less than 0.0005 W/W,[9] while wafer-fused NIR upconverter with InGaAs/InP photodetector and optimized GaAs/AlGaAs LED has an efficiency of 0.018 W/W.[10] It should be noted that above assessment of upconversion efficiency is reasonable for practical full GaAs-based NIR upconverters with both the *p-i-n* photodetector and the LED fabricated as a single device, since the used parameters (100% internal efficiency and 2% escaping probability) are indeed achievable for well-designed planar GaAs/AlGaAs LEDs.[10] What makes full GaAs-based upconversion more attractive is that the room-temperature upconversion efficiency is expected to increase further, through improvements such as utilization of resonant microcavity, fabrication of surface-textured LEDs, or direct mounting of the LED on a high reflective surface,[10] which are all well-established techniques for GaAs systems.

Finally, we present the relationship between the room-temperature upconversion efficiency and the incident laser intensity. As illustrated in Fig. 4(b), the upconversion efficiency has an obvious tendency to decrease with increasing light intensity. This phenomenon is more apparent for high reverse bias voltages, e.g., the upconversion efficiency at -7 V bias decreases from 0.048 to 0.011 W/W when the incident light intensity is increased from 12 to 335 mW/cm^2. Meanwhile, it stays more or less the same under low reverse bias voltages such as -4 or -5 V. This behavior is caused by the saturation of both the *p-i-n* photodetector and the LED. For a *p-i-n* detector, when the excitation is strong, charge tends to pile up; and for a LED under high current injection, a large fraction of carries diffuse/drift over the active region and recombine nonradiatively, resulting in a reduced emission efficiency. Note that we are using a laser illuminating the device directly. In a practical application, the power density is expected to be much lower.

This work was supported by the Natural Science Foundation of China under Contract Nos. 60576067 and 10734020, the National Minister of Education Program No. IRT0524 and Shanghai Municipal Key Project No. 08XD14022.

[1] J. S. Sandhu, A. P. Heberle, B. W. Alphenaar, and J. R. A. Cleaver, Appl. Phys. Lett. **76**, 1507 (2000).
[2] M. Chikamatsu, Y. Ichino, N. Takada, M. Yoshida, T. Kamata, and K. Yase, Appl. Phys. Lett. **81**, 769 (2002).
[3] K. J. Russell, I. Appelbaum, H. Temkin, C. H. Perry, V. Narayanamurti, M. P. Hanson, and A. C. Gossard, Appl. Phys. Lett. **82**, 2960 (2003).
[4] D. Ban, S. Han, Z. H. Lu, T. Oogarah, A. J. SpringThorpe, and H. C. Liu, Appl. Phys. Lett. **90**, 093108 (2007).
[5] P. W. Kruse, F. C. Pribble, and R. G. Schulze, J. Appl. Phys. **38**, 1718 (1967).
[6] Y. Mita, Appl. Phys. Lett. **39**, 587 (1981).
[7] Y. Wang and J. Ohwaki, J. Appl. Phys. **74**, 1272 (1993).
[8] H. C. Liu, M. Gao, and P. J. Poole, Electron. Lett. **36**, 1300 (2000).
[9] J. B. Héroux, X. Yang, and W. I. Wang, Appl. Phys. Lett. **75**, 2716 (1999).
[10] D. Ban, H. Luo, H. C. Liu, Z. R. Wasilewski, A. J. SpringThorpe, R. Glew, and M. Buchanan, J. Appl. Phys. **96**, 5243 (2004).
[11] T. Akatsu, A. Plössl, R. Scholz, H. Stenzel, and U. Gösele, J. Appl. Phys. **90**, 3856 (2001).
[12] M. Kondow, K. Uomi, A. Niwa, T. Kitatani, S. Watahiki, and Y. Yazawa, Jpn. J. Appl. Phys., Part 1 **35**, 1273 (1996).
[13] G. Ungaro, G. L. Roux, R. Teissier, and J. C. Harmand, Electron. Lett. **735**, 12466 (1999).
[14] J. C. Harmand, G. Ungaro, L. Largeau, and G. L. Roux, Appl. Phys. Lett. **77**, 2482 (2000).
[15] Q. Han, X. H. Yang, Z. C. Niu, H. Q. Ni, Y. Q. Xu, S. Y. Zhang, Y. Du, L. H. Peng, H. Zhao, C. Z. Tong, R. H. Wu, and Q. M. Wang, Appl. Phys. Lett. **87**, 111105 (2005).
[16] J. S. Ng, W. M. Soong, M. J. Steer, M. Hopkinson, J. P. R. David, J. Chamings, S. J. Sweeney, and A. R. Adams, J. Appl. Phys. **101**, 064506 (2007).
[17] H. Luo, J. A. Gupta, and H. C. Liu, Appl. Phys. Lett. **86**, 211121 (2005).
[18] K. H. Tan, S. F. Yoon, W. K. Loke, S. Wicaksono, T. K. Ng, K. L. Lew, A. Stöhr, S. Fedderwitz, M. Weiß, D. Jäger, N. Saadsaoud, E. Dogheche, D. Decoster, and J. Chazelas, Opt. Express **16**, 7720 (2008).
[19] I. Schnitzer, E. Yablonovitch, C. Caneau, and T. J. Gmitter, Appl. Phys. Lett. **62**, 131 (1993).